Vol. 2, No. 1 (2021); 3–19

**Journal of Earth Sciences and Technology**

http://www.htpub.org/Journal-Of-Earth-Sciences-And-Technology/

# Evaluation of SQp SQs Attributes for Hydrocarbon Reservoir Identification

Abdullah Ali El-Badaji[a]*, Maman Hermana[a]

[a]*Department of Geoscience, University Teknologi PETRONAS, 32610 Seri Iskandar, Malaysia*

**Article Information**

**Article History**
Received: 04/10/2021
Accepted: 15/10/2021
Available online: 17/10/2021

**Keywords**
Seismic
Attributes
SQp
SQs
AVO
Inversion

**Abstract**

*Identification of hydrocarbon formation is quite easily recognized on well log data using certain well log data including gamma-ray and resistivity log. However, to get 3D coverage based on these two logs is mostly impossible due to limited well numbers and costs. To overcome these difficulties, interpreters must use other equivalent data to gamma-ray and resistivity logs from seismic data, which in this case are the proposed AVO attributes SQp and SQs that are formulated from seismic-attenuation rock physics. Where SQp has a similar response with a gamma-ray log which eventually can be used for classifying/identifying facies and SQs response similar to resistivity log even in different reservoir conditions. This study will focus on testing these new attributes on real seismic data and compare them with the existing attribute, evaluate their effectiveness, and check which attribute is more sensitive to hydrocarbon identification.*

## 1. Introduction

The ultimate objective in the oil and gas industry is to find hydrocarbon (HC). Currently, the common method for hydrocarbon identification and reservoir recognition on well log data is using gamma-ray and resistivity logs (Hermana, 2018). But well logs are limited to a very small coverage area (only in wellbore location).

Another way for hydrocarbon identification outside the well location is through using seismic data. However, the attributes extracted from the seismic through seismic inversion and AVO analysis still have some limitations to optimize the finding of hydrocarbon. These limitations are such as ambiguity and pitfall in amplitude interpretation due to the dual effect of lithology and pore fill at the same time on the seismic data which means that not all bright spots are DHIs (Hermana, Ghosh, & Sum, 2016b).

* Corresponding author
*E-mail address:* abd9942@gmail.com

To overcome these difficulties, other methods need to be proposed to solve the problem. SQp-SQs attributes will be proposed to be tested on the selected field by implementing seismic inversion and AVO. And by applying these attributes we will have the advantage of SQp having a similar response with a gamma-ray log which is used as an indicator for lithology and SQs having a response similar to resistivity log which can be used as an indicator of pore fill (Hermana, 2018).

## 2. Methodology

The formation of hydrocarbon was identified firstly in well log data based on existing data. To identified the hydrocarbon delineation on 3D coverage, seismic data was used by integrating it with well log data on the various study including AVO forward modeling, AVO analysis, and seismic inversion. A feasibility study on well log data also has been conducted to see the sensitivity of developed attributes and comparison purposes on identifying hydrocarbon formation targets in the area. The available data set is including well log data and partial stack seismic data as required to perform the simultaneous inversion.

Based on the Gamma-Ray log, which is used as a lithology indicator, the well was divided into two facies which are sand and shale. Furthermore, by utilizing density, resistivity, and saturation logs, zones of high potential to be HC reservoirs have been identified to pursue further studies.

Fluid substitution modeling (FSM) was conducted to define what logs would look like with different quantities or types of certain properties within the area of interest. This technique modeling is used to evaluate wave velocity changes with the variation of the type of pore-fluid and its saturation either increasing or decreasing (Wawrzyniak-Guz, 2019).

To explore the parameters that have a strong correlation between petrophysics and seismic data, sensitivity analysis has been performed. On the seismic resolution scale, some parameters need to be shown in well domain before are applied to seismic inversion results. Those parameters are including the type of reservoir rock, hydrocarbon zone thickness (pay zone), fluid type in the reservoir, and petrophysical parameters such as porosity, saturation, and others by using the well log data (Hampson, 2004). By integrating the well data with seismic data, cross-plots were generated to evaluate the petrophysical parameters that correlate well with the seismic data. AVO modeling on the responses of FSM is conducted to measure the differences in seismic reflection amplitude with offset, AVO analysis help geophysicists to make a better assessment of the properties of the rock reservoir, including porosity, density, lithology, and fluid consistency (Feng & Bancroft, 2006).

Seismic-well-tie was conducted before seismic interpretation by interactive check-shot calibration of sonic log data, analytical wavelet creation, statistical and deterministic wavelet extraction, and finally synthetic seismogram generation for 2D and 3D seismic data (Avseth, Mukerji, & Mavko, 2005). Horizon picking was conducted in the targeted formation to generate surface maps, data slices as well as for well to seismic tie.

## 3. Results and discussion

### *3.1 Well Log Interpretation*

From the available logs and by utilizing GR, density, resistivity, and saturation logs reservoir has been identified at the depth of ≈ 1220-1232 ms (1215-1225 m) as shown in figure 1. The selected reservoir shows a relatively low GR with a cut-off value of 50% indicating clean sand, low density, and high resistivity indicates the presence of hydrocarbon and finally, the saturation log interprets the saturation of water in the reservoir which indicates high HC saturation.

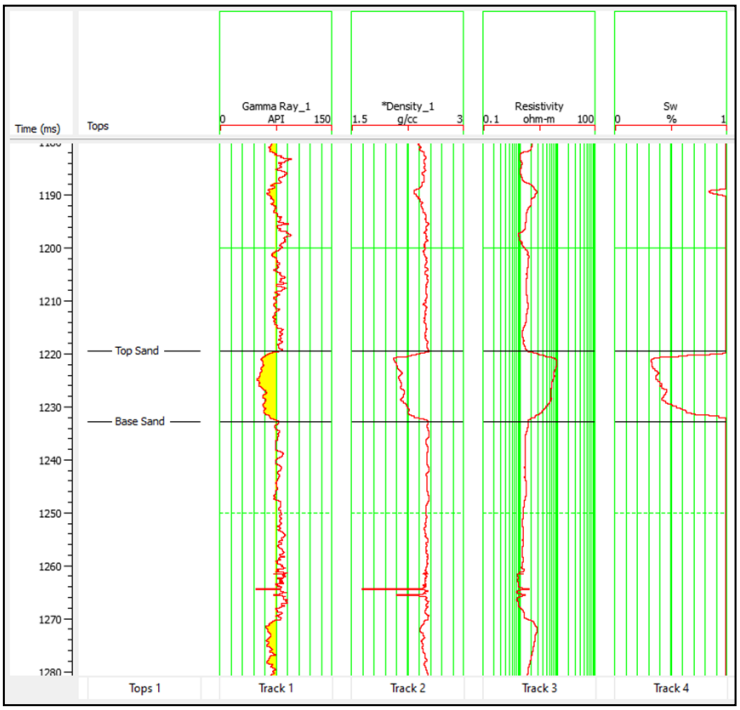


Fig. 1. Well log interpretation.

### *3.2 Fluid Substitution Modeling (FSM)*

Fluid substitution modeling has to be applied on a clean sand interval which in this case is the identified reservoir. FSM is applied in order to test the sensitivity of elastic properties to fluid change and their ability to identify hydrocarbons (Hermana et al., 2016). For this study, three scenarios have been performed which are 100% brine, 100% oil, and 100% gas.

FSM mainly changes Vp, Vs, and density which eventually change other elastic properties as they depend on these main parameters (Avseth et al., 2005). These elastic properties are such as Vp/Vs ration, P-impedance, S-impedance, Mu-Rho, Lambda-Rho, SQp, SQs, and Poisson ratio as illustrated in figures 2-4. And it is noticed that the wells that came out with good separation for all scenarios are Density, P-wave, P-impedance, Lambda-Rho, SQp, and SQs log.

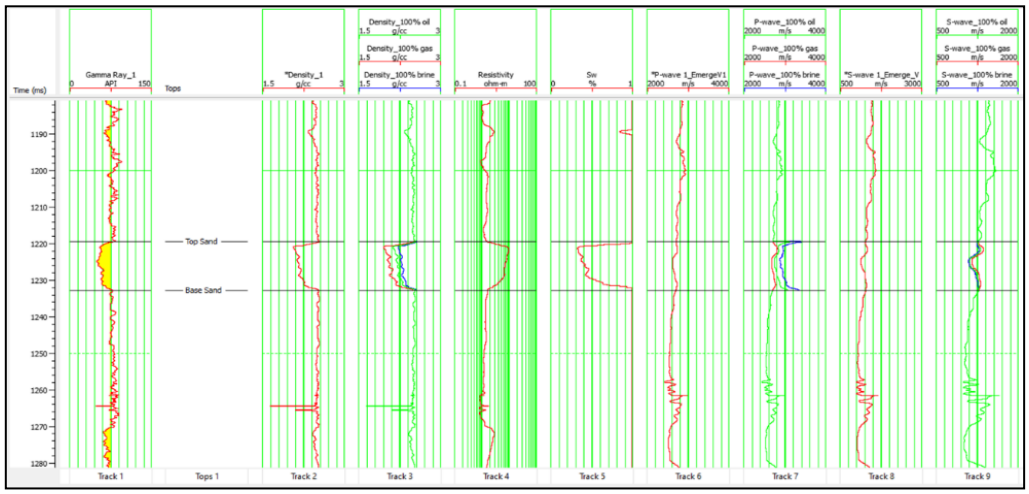


Fig. 2. FSM (Density, P-wave, and S-wave).

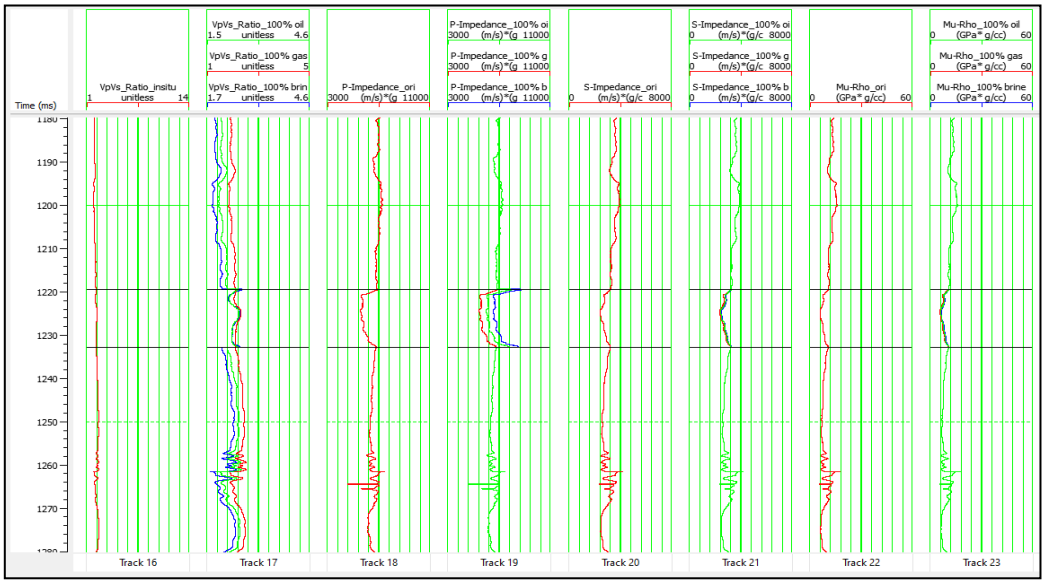


Fig. 3. FSM (Vp/Vs Ratio, P-impedance, S-impedance, and Mu-Rho).

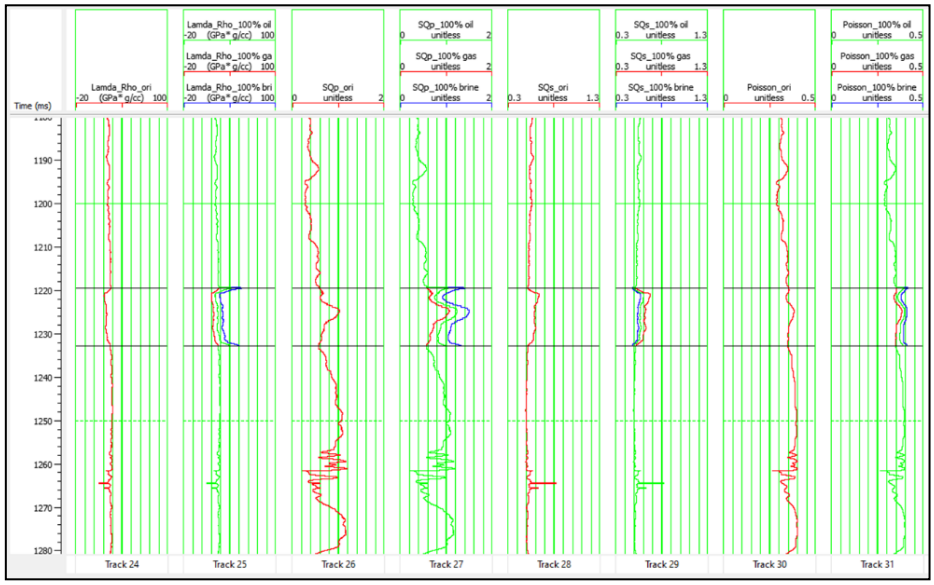


Fig. 4. FSM (Lambda-Rho, SQp, SQs, and Poisson Ratio).

### *3.3 Well feasibility study*

This stage is usually conducted on the reservoir or interval or interest using measured rock, fluid properties, and reservoir simulation model. These mentioned properties are obtained from the borehole (well log) data, core samples, laboratory measurement of fluid properties as well as tests (Prajapati et al., 2019). In this study, several cross-plots of elastic properties have been generated in order to find the best properties for hydrocarbon delineation.

*Poisson vs P-Impedance*

By using Gama-Ray as the color key, the distribution of lithology can be distinguished. And using the same range of value of gas scenario in FSM as shown in figure 5(a) to plot the gas zone in the Poisson vs P-Impedance cross-plot then showing the cross-section at the well, the following separation can be obtained.

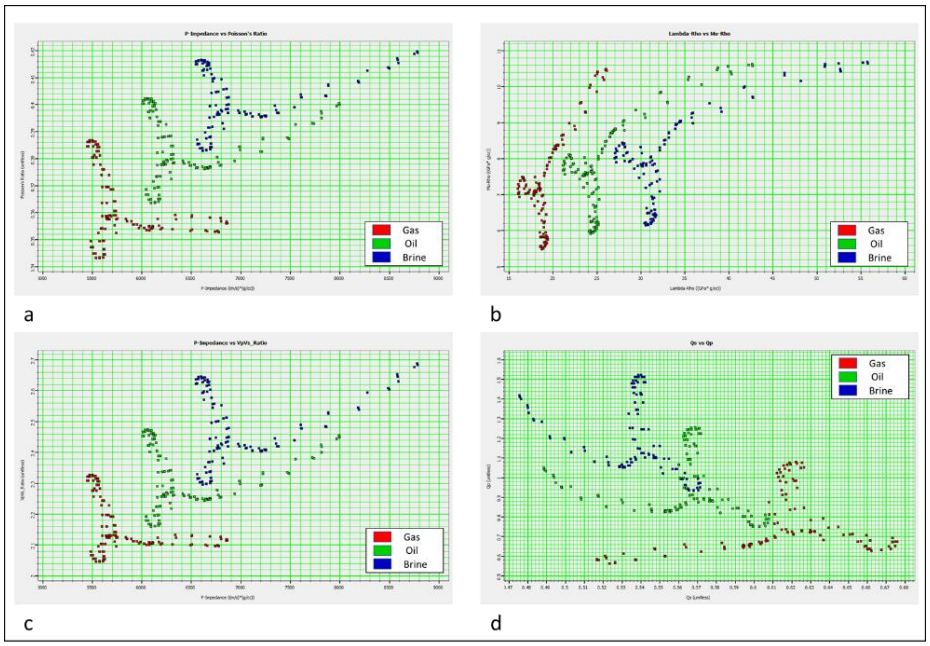


Fig. 5. Well logs FSM results from crossplots within the reservoir only. (a) P-impedance vs Poisson Ratio, (b) LMR, (c) P-impedance vs Vp/Vs, and (d) SQp vs SQs.

In addition, by using resistivity as the color key of the cross-plot, the gas zone can be identified by the area that exhibits high resistivities compared to brine sand and shale as shown in the figure 6 below.

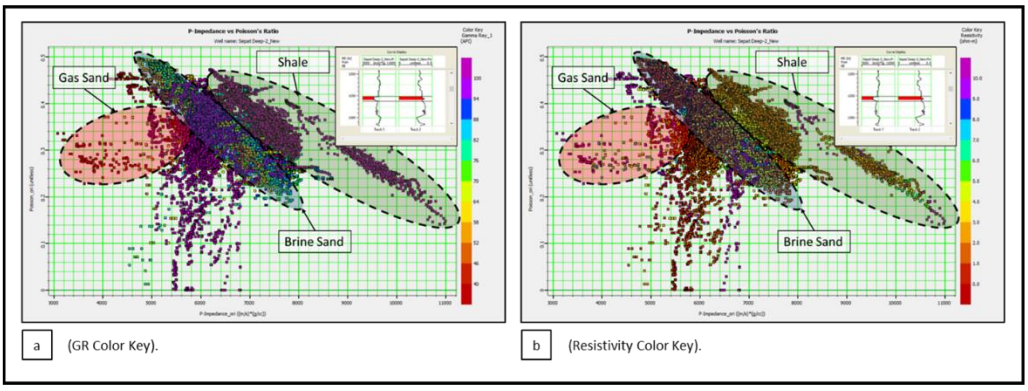


Fig. 6. Poisson vs P-Impedance.

*Mu-Rho vs Lambda-Rho*

Mu-Rho vs Lambda-Rho shows a good separation of different lithologies and fluids as shown in figure 5b and figure 7 and by using GR and Resistivity color keys, we can identify the area of gas sand which is represented by relatively low Mu-Rho and Lambda-Rho compared to brine sand and shale.

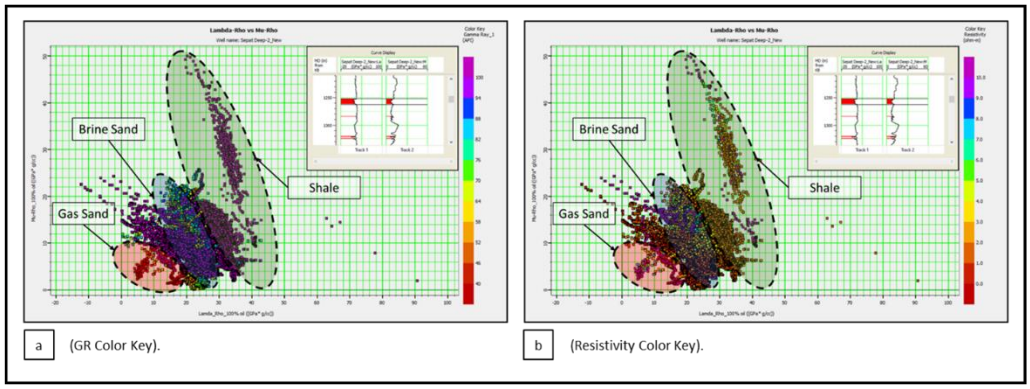


Fig.7. Mu-Rho vs Lambda-Rho.

*P-impedance vs Vp/Vs ratio*

As discussed for Mu-Rho vs Lambda-Rho, gas sand has low P-Impedance. In addition, gas sand has a low Vp/Vs ratio, and therefore it can be separated from brine sand which has a relatively high Vp/Vs ratio. Also, it can be separated from shale based on P-Impedance as shale has a notable higher P-Impedance than gas sand (Figure 5c and Figure 9).

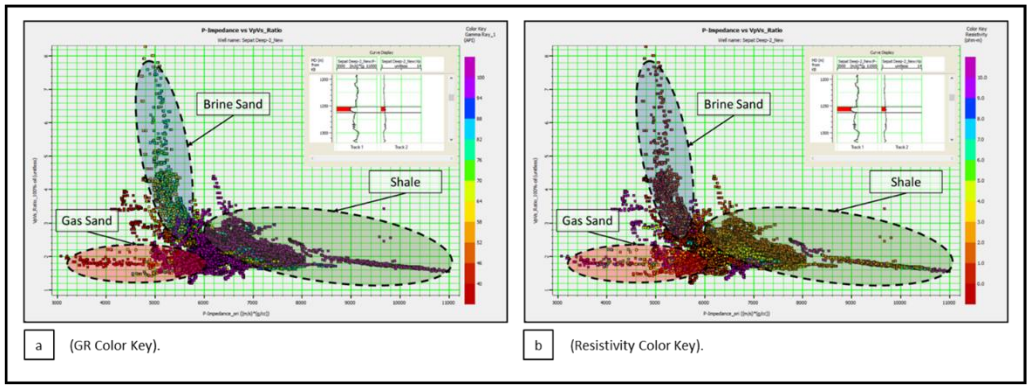


Fig. 8. P-Impedance vs Vp/Vs ratio.

*SQp vs SQs:*

It is known that gas sand has low GR response and high resistivity. SQp imitates GR log while SQs imitates resistivity log (Hermana et al., 2016a). Therefore, gas sand can be identified on the cross-plot based on SQp and SQ as shown in figure 5d and figure 9.

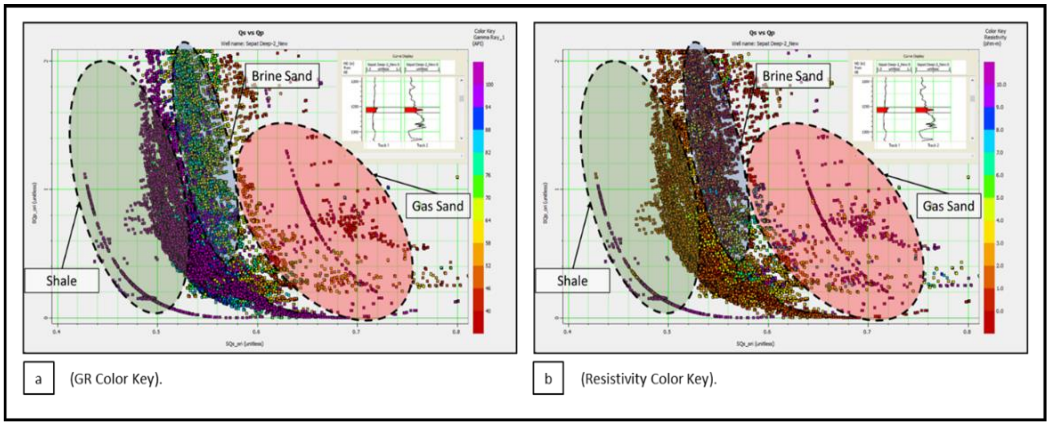


Fig. 9. SQp vs SQs crossplot.

*3.4 Synthetic seismogram and well tie*

Seismic to well tie is performed in order to correlate the well logs which is the in-depth domain to the seismic which is in the time domain and to achieve that we have to start with wavelet extraction.

There are several ways to extract the wavelets such as extraction from well or from seismic. For seismic to well tie a statistical wavelet has been extracted from the mid-angle stack seismic data as shown in figure 10.

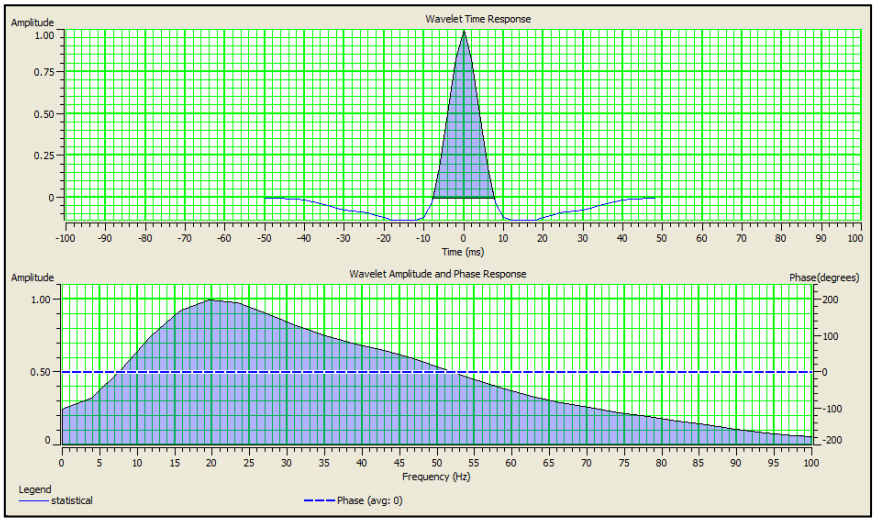


Fig. 10. Statistical wavelet from mid-angle stack seismic.

Moving toward correlation of the well to seismic data manual shifting of some events has been done in order to increase the correlation as well as correlating well tops to seismic horizons where applicable. A maximum correlation of 0.550 has been achieved which is fairly good; however, it can be noticed that the area of interest has an excellent well to seismic correlation as shown in figure 11.

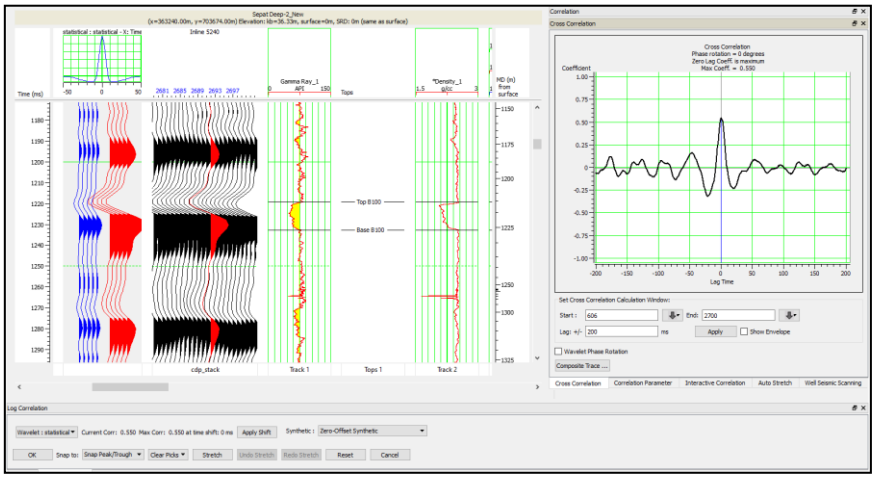

Fig. 11. Seismic to well correlation window.

### *3.5 Horizon picking*

A horizon has been picked using automatic picking. After QC of the auto-picked horizon, it shows a good fit at the area of interest. Furthermore, the selected horizon has been smoothed and interpolated to carry on this research and to be used for creating data slices (Figure 12).

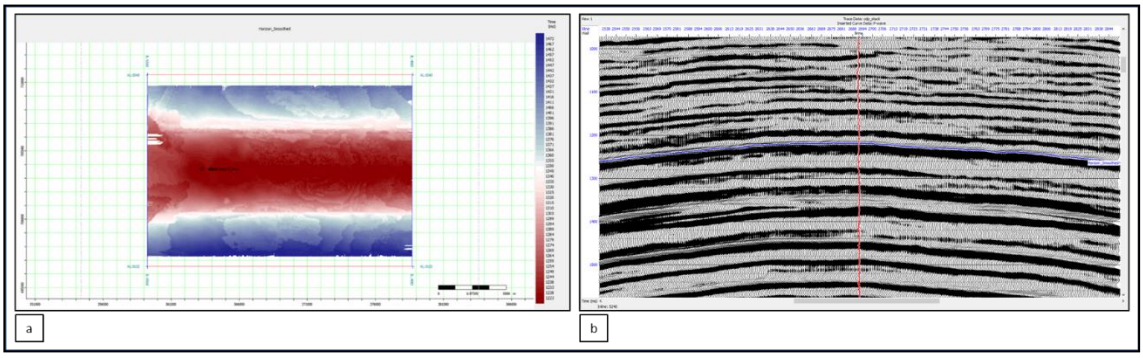


Fig. 12. Picked horizon: (a) surface map, (b) cross-section.

### *3.6 AVO modeling*

AVO method measures the difference in seismic amplitude with distance variations between the source and receiver (Feng & Bancroft, 2006). And from the gradient analysis, it has been found that the top of

gas sand in the reservoir of interest has a negative intercept and a positive gradient while on the other hand, the base of gas sand has a positive intercept and a negative gradient. figure 13 (a) shows the variation of amplitude with offset while figure 13 (b) shows the intercept and gradient of top and base of gas sand represented by red and black boxes respectively.

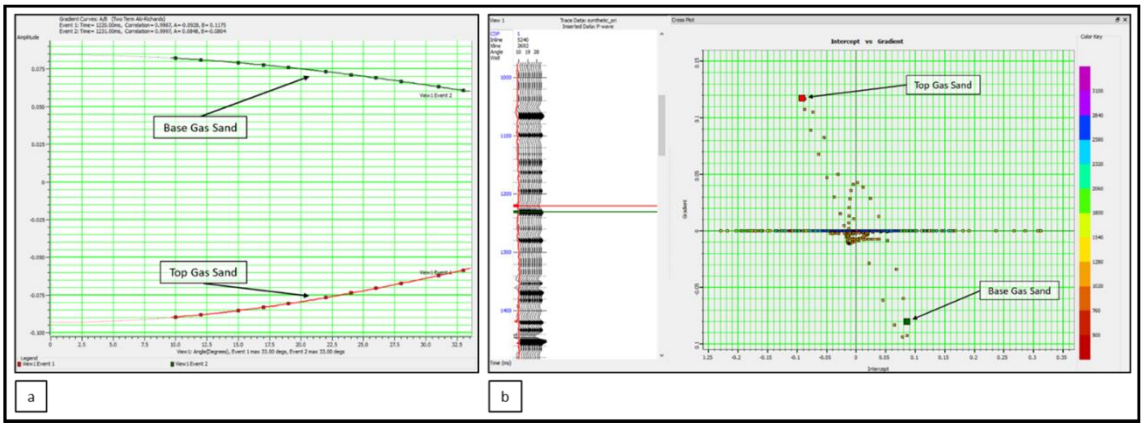


Fig. 13. (a) Amplitude variation with offset, (b) intercept and gradient cross-plot.

Additionally, by displaying the Scaled Poisson Ratio attribute it has been proved that the presence of gas decreases the Poisson ratio as displayed in figure 14 (a) in the cross-section. And by creating a surface map at the horizon with a window of 50 ms below it the distribution of HC can be interpreted as displayed in the map below in figure 14 (b).

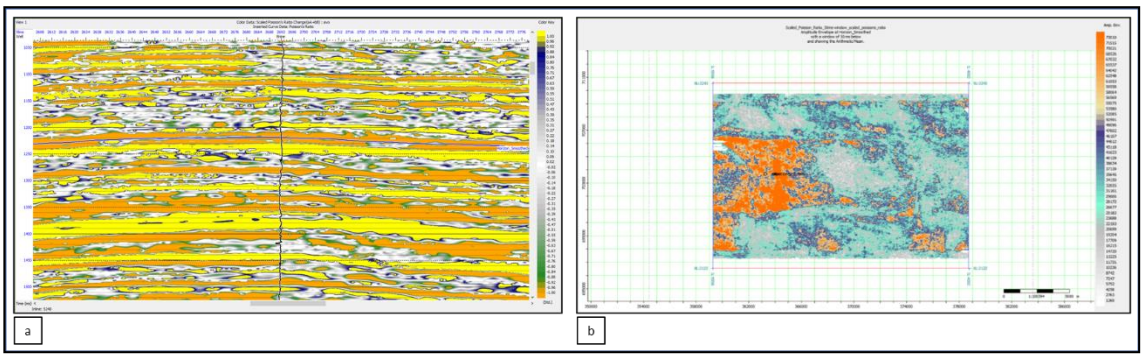


Fig. 14. AVO scaled poisson ratio: (a) cross-section, (b) data slice.

Another AVO attribute to indicate fluids is Fluid Factor. Which is given by the following equation (Hampson, 2004).

$$\Delta f = Rp - 1.16 \times \left(\frac{V_s}{V_p}\right) \times Rs \quad (1)$$

where (Vp/Vs = 2). Gas sand is interpreted to have a low fluid factor as shown in figure 15.

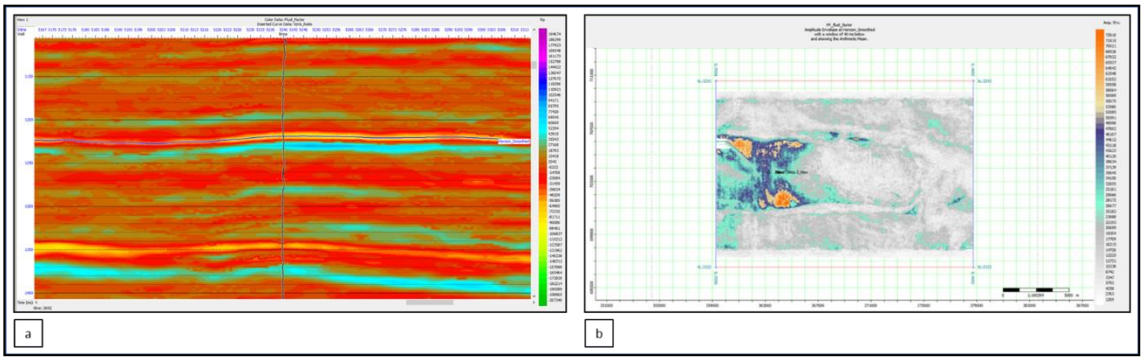


Fig. 15. Fluid factor: (a) cross-section, (b) data slice.

### *3.7 Seismic inversion*

In a seismic inversion, we have to go through several steps starting with wavelet extraction, model building, inversion analysis and finally applying to the volume.

#### *3.7.1 Extracting wavelet*

A group of wavelets has been extracted in order to perform inversion which is near, mid, and far that were extracted with angle ranges 5-15, 15-25, and 25-40 respectively. The above-mentioned wavelets are shown in figure 16.

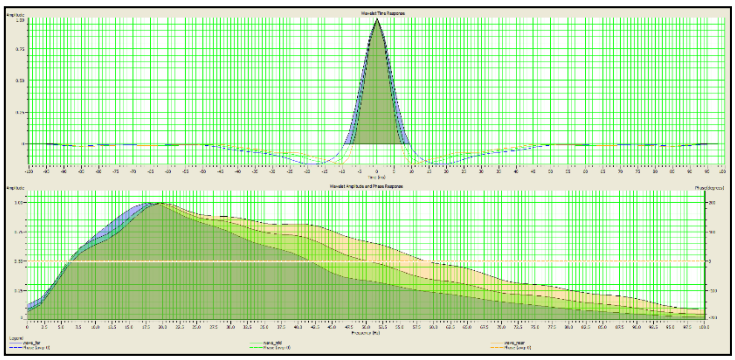

Fig. 16. Wavelet group used for inversion.

#### *3.7.2 Creating model*

At this stage, a simple model has been built representing the change in the wave shape of the signal as it passes through earth layers using the available well data and extrapolating it to the seismic volume. The generated models are shown in figure 17 with the related curve inserted for each model at the well location.

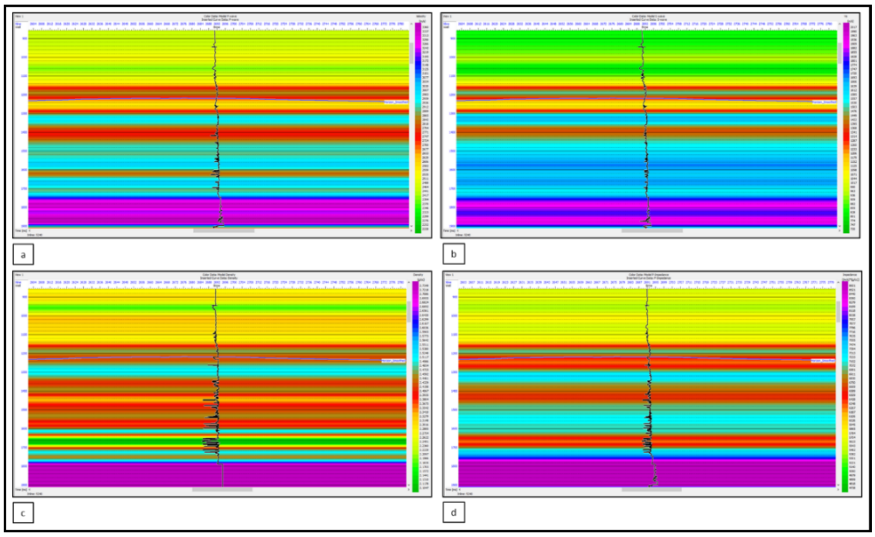


Fig. 17. (a) P-wave model, (b), S-wave model, (c) density model & (d) P-impedance model.

### *3.7.3 Inversion analysis*

Before applying inversion to the whole seismic volume, it is a good practice to test it first at the well location and if it shows a good fit (low error) then we can apply it to the whole volume. In this study, inversion analysis showed a good fit between the inverted model and the well as shown in figure 18.

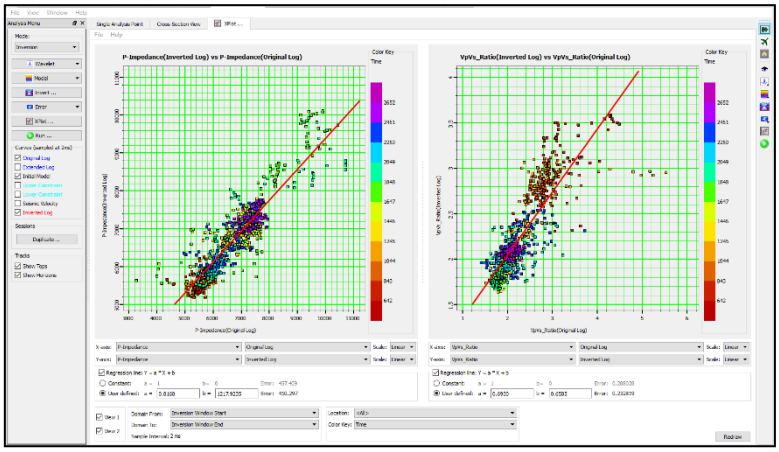

Fig. 18. Inversion analysis, (Left) inverted vs log P-impedance & (Right) inverted vs well Vp/Vs ratio.

### *3.7.4 Applying to the Volume*

The inversion has been applied to a cropped volume around the area of interest with Xline range (2591-2791) and Inline (5139-5339). The inverted models, then have been compared to the models

created from the well to QC the inverted data. Figure 19 shows the comparison between the inverted synthetic, gather the group and followed by the error plot from right to left respectively.

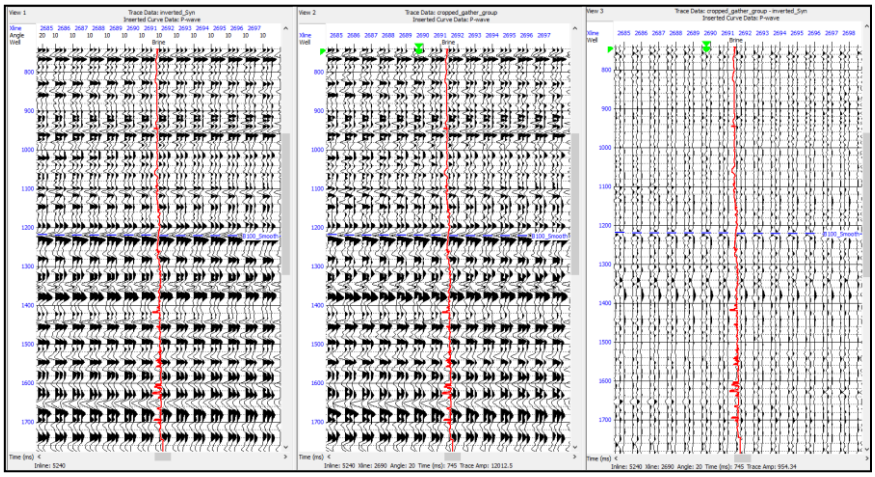

Fig. 19. From left to right (inverted synthetic, gather group, and error plot).

From the error plot (gather_group – inverted_syn) it is clear that the inverted data exhibits a minimal error. The following figures (Figure 20-25) will show the inverted models compared to the models generated from the well with each related curve inserted for QC purposes.

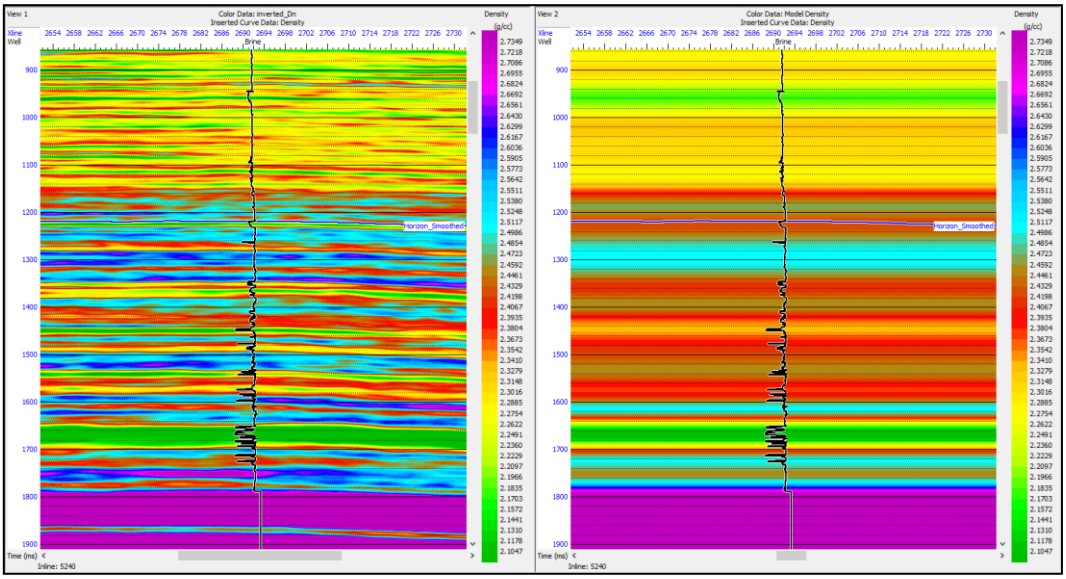

Fig. 20. Inverted Dn compared to density model.

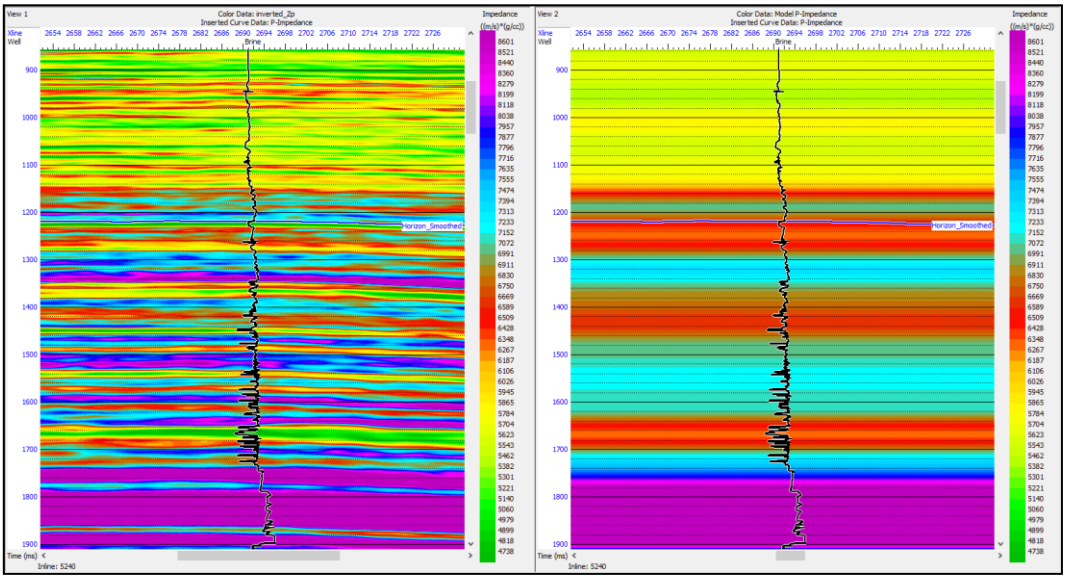


Fig. 21. Inverted Zp compared to P-Impedance model.

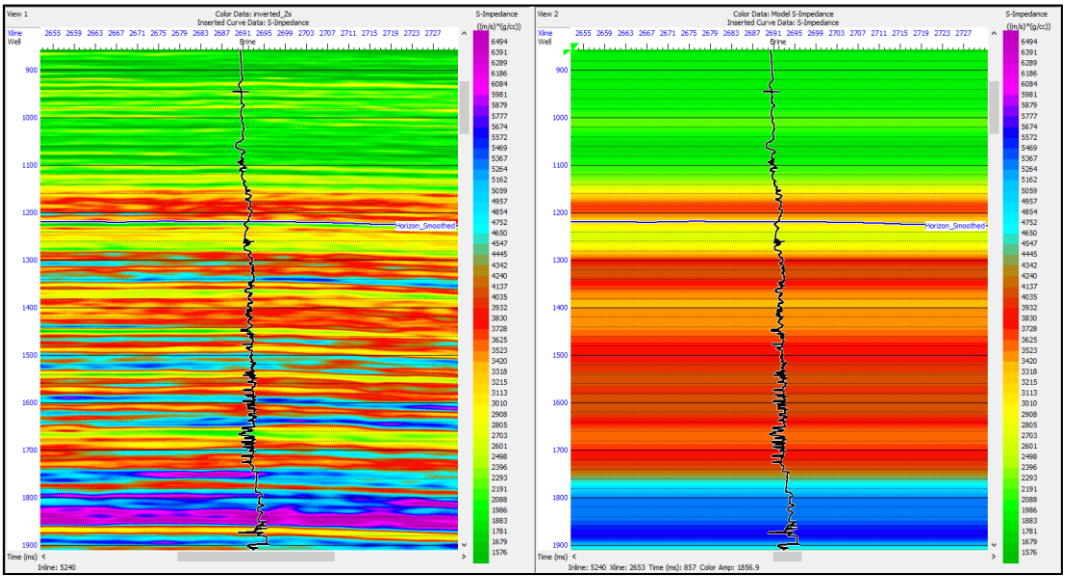


Fig. 22. Inverted Zs compared to S-impedance model.

Furthermore, using trace math, Inverted SQp and SQs have been calculated and surface maps at the horizon with the window of 40 ms below were generated to illustrate the facies distribution using SQp as it imitates GR and HC distribution using SQs as it imitates Resistivity.

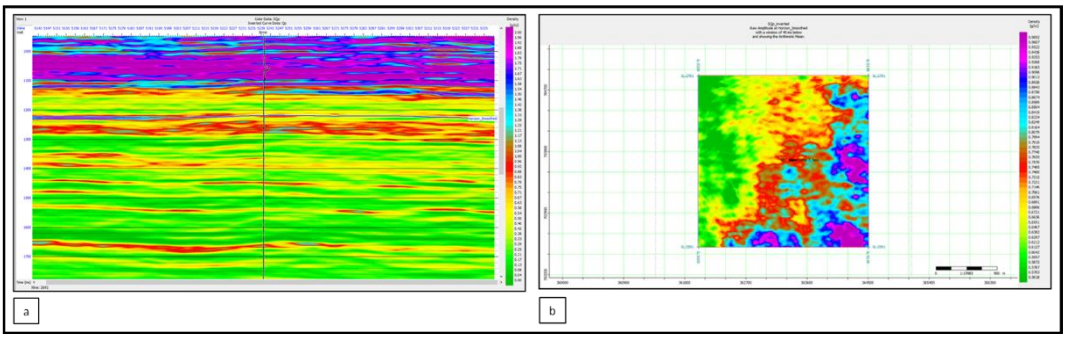


Fig. 23. Inverted SQp: (a) cross-section, (b) inverted SQp surface map.

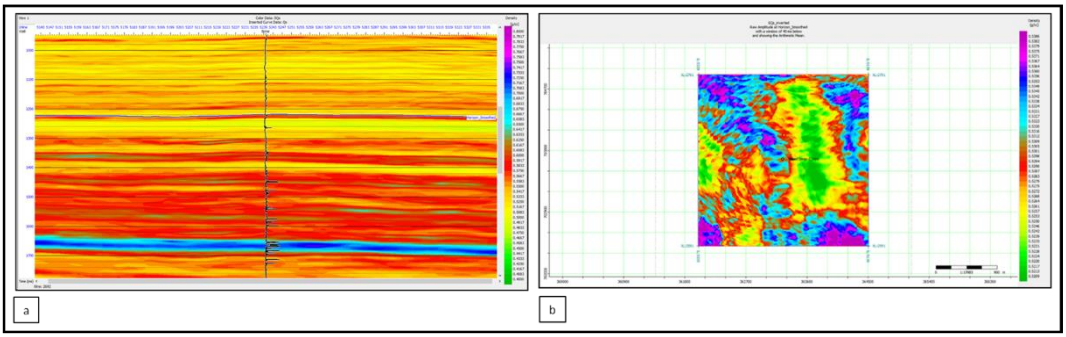


Fig. 24. Inverted SQs: (a) cross-section, (b) surface map.

Additional comparisons have been done by creating surface maps at the horizons such as Poisson ratio, P-Impedance, Fluid Factor, Lambda-Rho, and Mu-Rho to compare the distribution of hydrocarbon. Similar distributions of anomalies are observed from inversion results around the well location, which confirms the good quality of the inverted results.

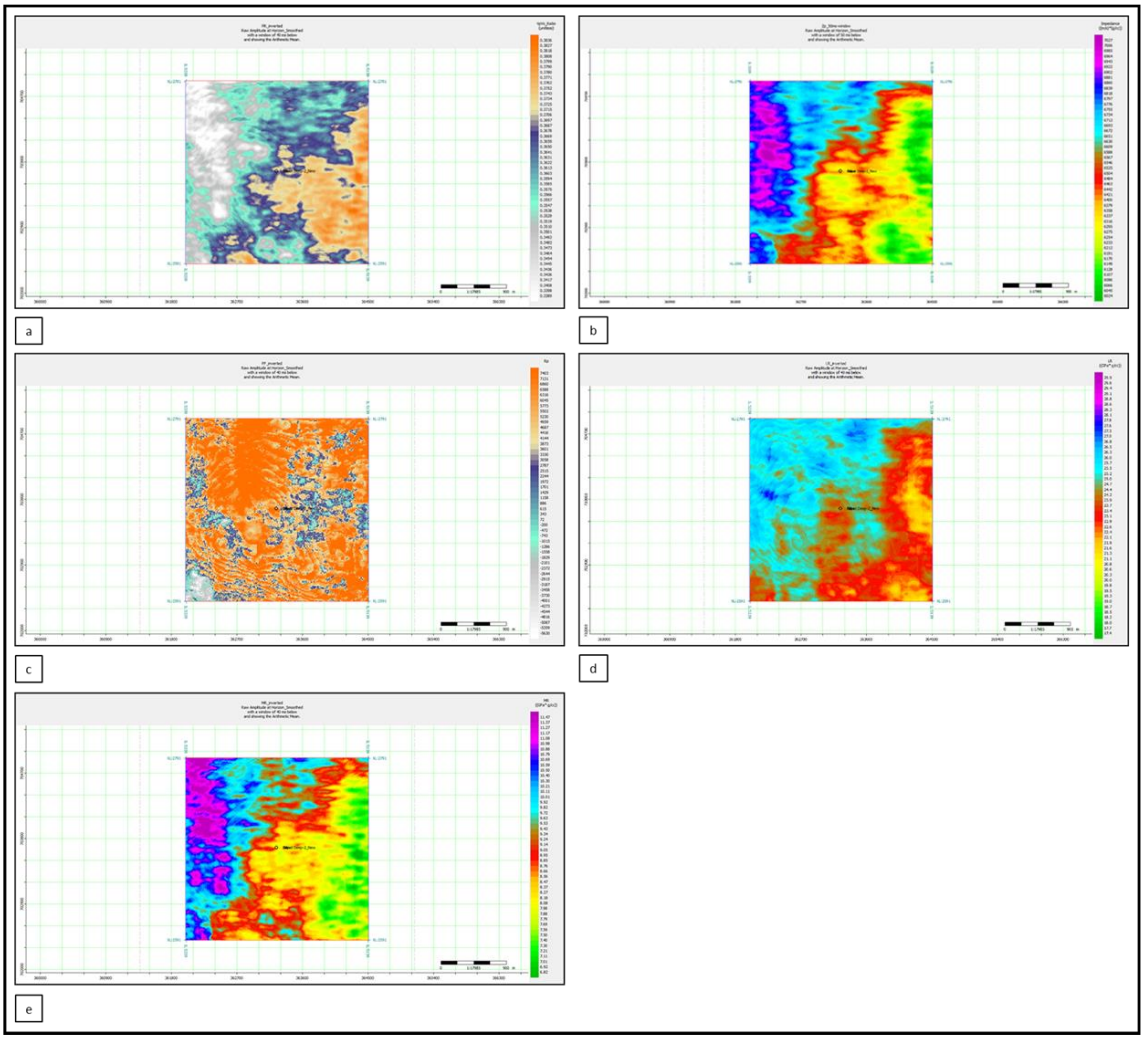


Fig. 25. (a) Inverted poisson ratio, (b) inverted P-impedance, (c) inverted fluid factor, (d) inverted Lambda-Rho & (e) inverted Mu-Rho.

## 4. Conclusion

In conclusion, the main objectives which are to test, compare and evaluate SQp and SQs have been achieved successfully. Testing SQp-SQs on well log data through forward modeling and analysis has proven that SQp's response has a similar response to GR log where SQs's response is similar to Resistivity log. Then, the proposed attributes have been compared with the existing attributes through AVO analysis showing fairly good results in delineating the top and base of gas sand. And finally, SQp-SQs were evaluated for HC identification and illustrate the HC distribution through seismic inversion.

## Acknowledgement

Greatest gratitude to Dr. Maman for his time and guidance throughout this project as well as Universiti Teknologi Petronas (UTP) for providing the essential support and tools and CGG for providing HRS software available in UTP.

## References

Avseth, P., Mukerji, T., & Mavko, G. (2005). *Quantitative Seismic Interpretation : Applying Rock Physics Tools to Reduce Interpretation Risk*. New York, USA: Cambridge University Press.

Feng, H., & Bancroft, J. (2006). *AVO principles, processing and inversion*, CREWES research report, Volume 18 (2006) .

Hampson, D. (2004). AVO Theory: Hampson-Russell Software Services Ltd. In: Calgary.

Hermana, M. (2018). Feasibility Study of SQp and SQs Attributes Application for Facies Classification. *Geosciences (Switzerland), 8*. doi:10.3390/geosciences8010010.

Hermana, M., Ghosh, D., & Sum, C. (2016a). *New fluid and lithology indicator from seismic and rock physics:Malaysian offshore case study*. SEG Technical Program Expanded Abstracts : 2836-2840.

Hermana, M., Ghosh, D., & Sum, C. (2016b). *Optimizing the Lithology and Pore Fluid Separation Using Attenuation Attributes*. Offshore Technology Conference (OTC), Kuala Lumpur, Malaysia.

Hermana, M., Lubis, L., Ghosh, D., & Sum, C. (2016). *New Rock Physics Template for Better Hydrocarbon Prediction*. Offshore Technology Conference (OTC), Kuala Lumpur, Malaysia.

Prajapati, S., Liu, C., & Ghosh, D. (2019). *Rock physics templates and anisotropy*. Paper presented at the SEG International Exposition and Annual Meeting, San Antonio, Texas, USA.

Wawrzyniak-Guz, K. (2019). Rock physics modelling for determination of effective elastic properties of the lower Paleozoic shale formation, North Poland. *Acta Geophysica, 67*(6), 1967-1989. doi:10.1007/s11600-019-00355-6